J. Phys. Ther. Sci. 34: 777–783, 2022

The Journal of Physical Therapy Science

Original Article

Young's moduli of subcutaneous tissues and muscles under different loads at the gluteal region calculated using ultrasonography

Kaoru Isogai, RPT, MS[1)*], Shogo Okamoto, PhD[2)], Takayuki Asaba, RPT[3)], Shogo Ogusu, RPT[4)], Yusuke Shimizu, RPT[5)], Takafumi Watanabe, RPT[6)], Yoji Yamada, PhD[7)]

[1)] *Department of Physical Therapy, Faculty of Health and Medical Sciences, Tokoha University: 1230 Miyakoda-cho, Kita-ku, Hamamatsu-shi, Shizuoka 431-2102, Japan*
[2)] *Department of Computer Science, Graduate School of System Design, Tokyo Metropolitan University, Japan*
[3)] *Department of Rehabilitation, Seirei Hamamatsu General Hospital, Japan*
[4)] *Department of Rehabilitation, Yamauchi Orthopedic Clinic, Japan*
[5)] *Department of Rehabilitation, Iwata City Hospital, Japan*
[6)] *Department of Rehabilitation, Seisei Rehabilitation Hospital, Japan*
[7)] *Department of Mechanical Systems, Graduate School of Engineering, Nagoya University, Japan*

Abstract. [Purpose] Young's modulus distributions for subcutaneous and muscle tissues in a large sample of healthy individuals, based on ultrasonography and compression testing, remains uninvestigated till date. This study aimed to separately estimate the hardness of subcutaneous tissues and muscles in the human gluteal region under a range of loads in terms of mean Young's moduli and associated distributions. [Participants and Methods] Data of 21 males aged 20–22 years were acquired using synchronous compression testing and ultrasonography. Stress-strain curves comprised the loads applied (stress) were plotted against ultrasonographic changes in subcutaneous/muscle tissue thickness (strain). Young's moduli were calculated as slopes of approximation curves fitted to highly linear regions of the stress-strain curves. [Results] Young's moduli (mean ± standard deviation) for gluteal subcutaneous and muscle tissues were estimated as: 26.1 ± 19.0 kPa, 1-N load; 2,199.1 ± 1,354.8 kPa, 30-N load; and 62.2 ± 10.3 kPa, 5-N load; 440.4 ± 80.0 kPa, 30-N load, respectively. No correlation between any pair of these measures reached statistical significance. [Conclusion] Young's moduli were successfully measured for subcutaneous and muscle tissues in a large participant sample using ultrasonography and compression testing. Our results may serve as reference data when assessing tissue hardness by palpation.

Key words: Biological tissue, Stress-strain curve, Young's moduli

(This article was submitted Jul. 15, 2022, and was accepted Sep. 14, 2022)

INTRODUCTION

Palpation is a typical component of clinical assessments used to evaluate the hardness and other elastic properties of biological tissues. Clinicians need knowledge about the hardness of healthy human tissues to serve as a reference when comparing the extent to which patients' tissues are displaced under varying degrees of active compression. Distinguishing hardness between different healthy tissues is especially essential for physical therapists and other specialists who frequently deal with musculoskeletal diseases, as palpating muscle involves palpating the intervening subcutaneous tissue. Clinicians

*Corresponding author. Kaoru Isogai (E-mail: kisogai@hm.tokoha-u.ac.jp)

rely on subjective judgments of "healthy" tissue hardness based on their own experiences but would be aided by specific, quantifiable, and objective reference values.

Past attempts to quantify tissue hardness in humans have traditionally used compressive, indentation-based systems[1–16]. For example, Komiya et al. developed an instrument in which a force sensor was attached to the tip of a probe arm with a built-in potentiometer, and used it to measure pressure-displacement curves of the upper arm and forearm[3]. Morozumi et al. developed a tissue hardness meter with two pressure sensors corresponding to an inner, cylindrical shaft and outer, circumferential sheath, and tested its reliability in measuring hardness changes in the femoral region associated with muscle contraction[15]. Since these systems apply pressure from above the skin, they can quantify tissue hardness in aggregate, but they are not suited for measuring the hardness of subcutaneous and muscle tissues separately.

More recent attempts have focused on tomographic imaging technologies as a means to measure hardness separately in different body tissues[17–30]. For example, Uffmann et al. used magnetic resonance elastography to measure the shear moduli of the biceps brachii, flexor digitorum profundus, soleus, and gastrocnemius[21], while Chino et al. tested the reliability and validity of ultrasound elastography in quantifying the hardness of the human medial gastrocnemius[24]. However, the elastic moduli reported by those authors were calculated based on the wavelengths and velocities of vibrations propagating inside tissues. Since palpation is essentially compressive, such reference values would be more useful if derived based on the same measurement principle, i.e., from the slopes of force-displacement and/or stress-strain curves. Furthermore, stiffness measurements obtained by shear-wave ultrasound elastography have been found to only moderately agree with those obtained by indentation-based hardness meters, reaching correlations of just up to 0.5[30].

Force-displacement and/or stress-strain curves can be obtained if tomographic imaging and compressive loading are synchronized. Zheng et al. developed a device that combined an ultrasound transducer and load cell; from the force-displacement curves obtained, they calculated Young's moduli for lower limb soft tissues according to the site, posture, participant, and gender. However, they did not calculate them separately for subcutaneous and muscle tissues[31]. Elsewhere, Then et al. derived separate force-displacement curves for the subcutaneous tissue and muscle layers of human gluteal tissue and calculated respective shear moduli based on data obtained using a magnetic resonance imaging (MRI) device with an MRI-compatible loading device[32]. However, their curves were created based on only seven data points from a single participant. Notably, tissue-specific patterns of non-linear behavior were evident in their force-displacement curves, and the extent to which the subcutaneous layer was displaced was dependent on the degree of compressive force applied, yet also distinct from muscle's behavior under the same loads. Nevertheless, the authors' investigation paid little attention to hardness changes in response to incremental loading[32].

Because subcutaneous tissue and muscle hardness values are assumed to vary among even healthy individuals, determining separate hardness statistics for these two tissue layers in a healthy population (e.g., mean values and distributions) would yield useful reference data for detecting abnormalities in them by palpation. Furthermore, clinicians use palpation for diverse purposes and by means of different techniques. Given the non-linear behavior of subcutaneous tissues and muscles, being able to access reference data for hardness and strain over a wide range of loads would help them assess patients regardless of the clinical setting. Methodologically speaking, ultrasound tomography offers benefits at the sample level because sections can be acquired in shorter times compared with MRI, as well as the individual level because plenty of sections can be obtained in a single session with minimal burden.

The present study combined an ultrasound scanner and compression testing machine to determine distinct stress-strain curves for the subcutaneous and muscle layers of the human gluteal region. These data were used to derive mean values and distributions of Young's moduli in the two tissue layers under different loads along with associations between them. No research to date has investigated Young's moduli distributions for subcutaneous and muscle tissues in a large sample of healthy individuals using such a combination.

PARTICIPANTS AND METHODS

Twenty-one male university students without damage or disease in the gluteal region (age range, 20–22 years; height [mean ± standard deviation {SD}], 170.5 ± 4.5 cm; weight [mean ± SD]: 60.8 ± 8.7 kg; BMI [mean ± SD], 20.9 ± 2.2 kg/m^2) were screened for this study. Each participant provided written informed consent after receiving an explanation of the study aim and details. This study was approved by the Research Ethics Committee of Tokoha University (approval number: 2014-015H).

Our system combines an ultrasound machine (NEMIO SSA-550A; Toshiba Medical Systems Corp., Tokyo, Japan) with a compression testing machine (SV-52NA; Imada Seisakusho Co., Ltd., Toyohashi Aichi, Japan). The ultrasound probe was fastened to the compression machine using an extension arm, and the probe was oriented vertical to the ground. The contact area between the probe and skin was 576 mm^2 (W×D, 48×12 mm). The compression machine moved the arm in vertical direction.

The part of the left buttocks where the gluteus maximus and gluteus medius overlap was selected as the measurement site. Here, the muscle is plentiful, nearly flat, and supported by the lateral aspect of the iliac crest, allowing the displacement of both tissue layers to be stably observed over the course of incremental compression steps. Participants lay prone on a bed

with their right hip tilted downward at 50° such that the lateral aspect of their left iliac crest was parallel to the ground, and they were immobilized in this posture using the bed and a cushion (Fig. 1).

The probe was positioned at the midpoint of the anterior superior iliac spine and posterior superior iliac spine. Loads applied by the probe ranged from 0 to 45 N. In a previous study, we discovered that gluteal tissues start to rapidly harden at certain load levels, up to 3 N for subcutaneous tissue and up to 10 N for muscle, and that both subcutaneous tissue and muscle exhibit nearly linear behavior, at least before a 45-N load is applied[33]. Therefore, load increments were set to be finer at smaller loads and larger with increasing pressure. Thus, the following 14 load levels were tested in each imaging session: 0, 0.5, 1, 2, 3, 5, 7, 10, 15, 20, 25, 30, 35, and 45 N. The probe was lowered at a speed of 100 mm/min (1.67 mm/s) and halted manually once the pressure reading reached each target value. Ultrasonogram data were acquired and saved in parallel. On average, it took up to 15 minutes per participant to acquire the 14 ultrasonograms. Each participant was advised that if he felt pain in the gluteal region during compression, he could stop the compression machine's operation using the emergency abort button. However, no participant needed to press the button during the experiments.

Subcutaneous tissue thickness and muscle thickness were measured based on the complete series of ultrasonograms as the distance from the skin surface to the fat/muscle boundary and the distance from the fat/muscle boundary to the bone surface, respectively (Fig. 2a–d). Stress was calculated as the load applied by the probe divided by the area of probe-skin contact; strain was calculated based on the change in tissue thickness between the loads. For each of the 16 participants, separate stress-strain curves were plotted for the subcutaneous and muscle layers based on the values obtained. For the subcutaneous layer, Young's moduli under 1 N and 30 N loads were derived as the slope of the approximation curve fitted to the stress-strain

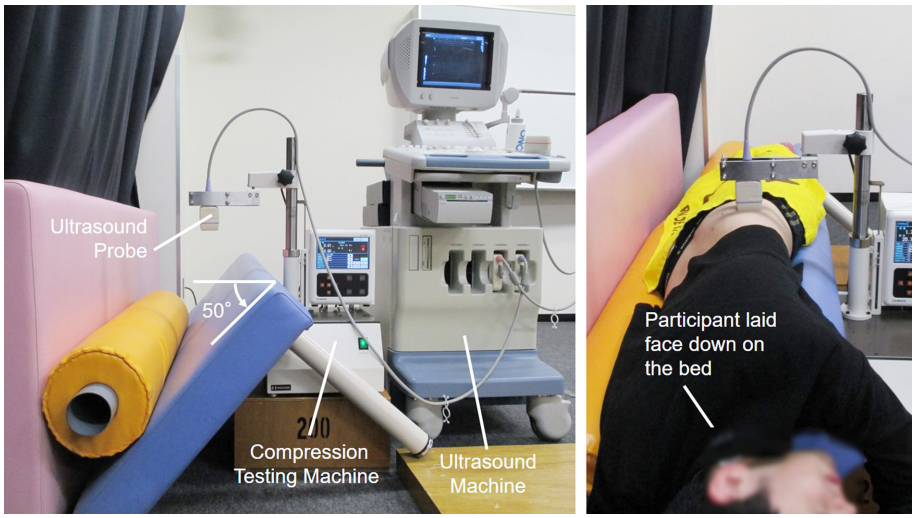

Fig. 1. Bed setting for measuring the hardness of human gluteal tissues and the ultrasound probe installed on the loading equipment.

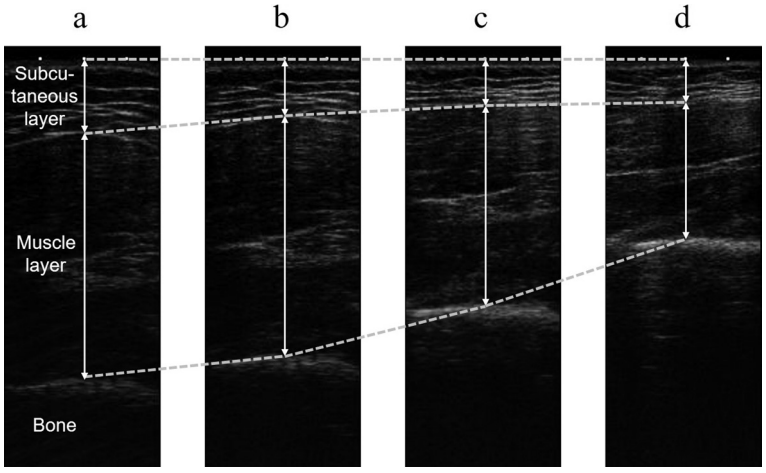

Fig. 2. Representative ultrasonograms of the subcutaneous and muscle layers of the human gluteal region. Each image was taken when the gluteal surface was pressed by the probe with compressive force values of 0 (a), 1 (b), 5 (c), and 30 N (d).

curve over the load ranges of 0–3 N and 15–45 N, respectively. For the muscle layer, Young's moduli under 5 N and 30 N loads were derived as the slope of the approximation curve fitted to the stress-strain curve over the load ranges of 0–10 N and 15–45 N, respectively. Each approximation curve was derived as a cubic polynomial. We selected these load ranges because the corresponding stress-strain curves were highly linear over these regions.

Four Young's moduli–i.e., subcutaneous tissue at 1 N, subcutaneous tissue at 30 N, muscle tissue at 5 N, and muscle tissue at 30 N–were tested for associations using Pearson's correlation analysis. Approximation curves and Pearson's R coefficients were calculated using Excel 2016 (Microsoft Corp., Redmond, WA, USA). Correlation strength was interpreted using the nomenclature advised for medical research by Akoglu[34].

RESULTS

Data from five of the 21 participants were excluded from the analysis because subcutaneous tissue and muscle displacement appeared disrupted (discontinuous) across consecutive images (n=2) or because the boundary between fat and muscle was indistinct in some images (n=3). The baseline values (mean ± SD) obtained for subcutaneous tissue and muscle thickness (i.e., in the unloaded state) for the remaining 16 participants were 12.6 ± 4.7 mm and 55.5 ± 7.6 mm, respectively.

Figure 3a, 3b shows the respective stress-strain curves of the subcutaneous and muscle layers acquired from each participant. These curves exhibit the typical non-linear behavior expected of biological tissues: Young's moduli appear to be smaller at lower loads and larger at higher loads. Overall, the stress-strain curves of the subcutaneous layer are nearly linear over the stress range of 0 up to 3 kPa, then curvilinear up to 10 kPa, but return to linear behavior at higher stresses. On the other hand, the stress-strain curves of the muscle layer are linear from 0 up to 10 kPa stress, then gently curvilinear up to 30 kPa, but return to linear behavior at higher stresses.

Hardness (i.e., Young's modulus) and strain values for each layer are presented in Table 1. For the subcutaneous layer, Young's moduli (mean ± SD) at 1 and 30 N were 26.1 ± 19.0 kPa and 2,199.1 ± 1,354.8 kPa, respectively; the respective strain values were 0.16 ± 0.05 and 0.33 ± 0.09. For the muscle layer, Young's moduli (mean ± SD) at 5 and 30 N were 62.2 ± 10.3 kPa and 440.4 ± 80.0 kPa, respectively; the respective strain values were 0.19 ± 0.03 and 0.47 ± 0.04. A correlation matrix of the four hardness measures is shown in Table 2. No correlation between any pair reached statistical significance.

DISCUSSION

Numerous studies have reported hardness data for subcutaneous and muscle tissues as well as corresponding Young's moduli, estimating these quantities using various methods. For example, Gefen et al. calculated Young's moduli ranging from 27 to 39 kPa for subcutaneous tissue in the plantar region based on MRI data[17], while Hai et al. reported a mean modulus of 15.9 kPa for subcutaneous tissue in the biceps brachii region based on photoacoustic elastography data[27, 28]. Compression or indentation devices have been used by teams including Horikawa et al., who reported a Young's modulus of 34 kPa for

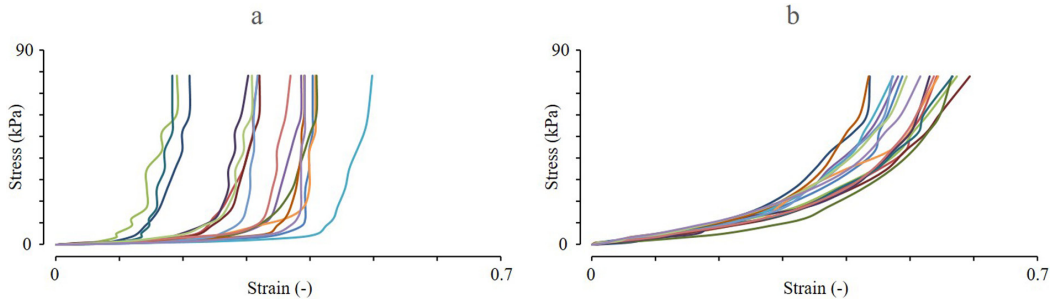

Fig. 3. Stress-strain curves of subcutaneous (a) and muscle (b) tissues for all participants. The results of the same participant are shown using the same line color in graphs a and b.

Table 1. Hardness and strain of subcutaneous and muscle tissues under variable loads

	Load (N)	Young's modulus (kPa)	Strain (-)
		Mean ± SD	Mean ± SD
Subcutaneous tissue	1	26.1 ± 19.0	0.16 ± 0.05
	30	2,199.1 ± 1,354.8	0.33 ± 0.09
Muscle	5	62.2 ± 10.3	0.19 ± 0.03
	30	440.4 ± 80.0	0.47 ± 0.04

Table 2. Correlation matrix for Young's moduli of subcutaneous and muscle tissues under variable loads

	a	b	c	d
a. Subcutaneous tissue hardness under 1 N load	1			
b. Subcutaneous tissue hardness under 30 N load	−0.33	1		
	(t=−1.323)			
	(p=0.207)			
c. Muscle hardness under 5 N load	−0.02	−0.07	1	
	(t=−0.074)	(t=−0.262)		
	(p=0.942)	(p=0.797)		
d. Muscle hardness under 30 N load	−0.17	0.18	0.26	1
	(t=−0.658)	(t=0.666)	(t=1.006)	
	(p=0.521)	(p=0.517)	(p=0.332)	

the deltoid at rest[2], and Komiya et al., who reported hardness values ranging from 18.8 to 30.4 kPa in the biceps brachii at different elbow angles[3]. Basford et al. have estimated muscle hardness using magnetic resonance elastography, and reported the following values: tibialis anterior, 35.6 kPa; gastrocnemius (medial head), 73.6 kPa; gastrocnemius (lateral head), 47.8 kPa; and soleus, 49.6 kPa[20]. Since some of these values were published as transverse coefficients, we have converted them to longitudinal equivalents assuming a Poisson ratio of 0.48, roughly the median of the values used by past studies[3, 4, 27, 28, 31]. In the present study, we estimated Young's moduli of 26.1 kPa in subcutaneous tissue under a 1-N load (1.7 kPa stress) and 62.2 kPa in muscle tissue under a 5-N load (8.7 kPa stress). Our estimates fall within the range of values reported in the aforementioned literature, despite being obtained under light loads and for a different body part.

Then et al. published force-displacement curves for subcutaneous and muscle tissues in the gluteal region acquired via simultaneous MRI and indentation loading[32]. Direct numerical comparison is difficult, but at least as far as can be visually confirmed, their force-displacement curves largely resemble our stress-strain curves. Furthermore, our stress-strain curves exhibit similar non-linear behavior to the force-displacement curves for biological tissue reported in past studies, evidencing smaller slopes under lighter loads but larger slopes under heavier loads[2, 3, 10, 14, 17, 31]. Such resemblances support the validity of our Young's moduli observed under a 30-N load (52.1 kPa stress) being dramatically larger than that under lighter loads (subcutaneous tissue [1-N load]: 2199.1 versus 26.1 kPa, muscle tissue [5-N load]: 440.4 versus 62.2 kPa). The corresponding coefficients reported by Then et al. for the gluteal region were 3.53 kPa (subcutaneous tissue) and 3.1 kPa (muscle tissue). However, as the authors themselves noted in their discussion, these are long-term elastic moduli, acquired after allowing tissue to fully relax under compression, preventing simple comparison with data from other literature.

The stress-strain curves we obtained for gluteal subcutaneous tissue are linear in the stress range of 0 up to 3 kPa, and the mean modulus over this interval was smaller than that of muscle. Let us assume a two-layer tissue structure: an upper subcutaneous layer and a lower muscle layer, each having different elastic properties. It stands to reason that subcutaneous tissue hardness would be easier to evaluate when this layer is softer than the underlying muscle layer than vice versa; in the first case, muscle displacement would be negligible, whereas in the second case, it would be the dominant component. Therefore, when palpating the subcutaneous layer of the gluteal region, we recommend that clinicians use compressive force corresponding to stress less than up to 3 kPa.

Over the stress range of 3–10 kPa, the subcutaneous tissue and muscle stress-strain curves have nearly identical slopes. Further, individual variation is evident in those curves' shapes. Clinicians should be advised that compressive force corresponding to stress in this range are likely to be unsuitable for evaluating hardness separately in the subcutaneous and muscle layers by palpation.

Our subcutaneous stress-strain curves were linear at stresses over up to 10 kPa, and the mean modulus over this interval was larger than that of muscle. It stands to reason that muscle hardness would be easier to evaluate when this layer is softer than the subcutaneous tissue above it than vice versa: in the first case, subcutaneous tissue displacement would be negligible, whereas in the second case, it would be the dominant component. Hence, when palpating the muscle layer of the gluteal region, we recommend that clinicians use compressive force corresponding to stress greater than up to 10 kPa at least in the range of 78.1 kPa or less, corresponding to the maximum load level tested in the present study (45 N).

Our results provide evidence of individual variation in subcutaneous tissue and muscle hardness, indicating that clinicians should compare what they feel when palpating a patient's body part with other healthy regions of the patient's body, such as the same area on the contralateral side, in addition to their sense of "average" hardness acquired via clinical experience. Furthermore, significant correlations were not observed for subcutaneous tissue hardness with muscle hardness under the same or different loads, and hardness of either tissue did not significantly correlate with itself under a different load. This variability highlights the importance of distinguishing between the subcutaneous and muscle layers during palpation, examining both under a range of compressive forces. If clinicians make judgments by palpating at a constant pressure or based on just one of these tissues, they risk missing the complete presentation of the gluteal region, to which each layer contributes.

The fact that boundaries between tissues were determined by visual inspection raises some doubts about the detection accuracy of our technique; although their locations on ultrasonograms were agreed on between the authors, they were not confirmed by a third party. The presence of ultrasound gel may also have affected our results. Gel must be applied to the measurement site for imaging but has non-zero weight and contact pressure; especially in the low-stress range tested herein, these factors may limit the accuracy of our stress-strain curves. Furthermore, biological tissue's hardness is closely linked to its viscoelastic properties; since our estimates were obtained by lowering the probe at a constant, slow rate (1.67 mm/s), they may not adequately reflect tissue hardness as encountered during palpation, in which compression is applied more quickly. Finally, the relationship of gluteal tissue hardness with the hardness of other body parts is unclear. Further, the relationship between the results of this study and the hardness felt by clinicians remains to be studied in the future.

In conclusion, we identified different stress-strain properties of the subcutaneous and muscle layers of the human gluteal region, and derived mean Young's moduli as well as distributions for each tissue under variable stress. Correlations between subcutaneous tissue and muscle hardness, either under the same stress or different stresses, were not observed, and the hardness of either tissue did not correlate with itself at different stresses. Our results are expected to serve as reference data for clinicians when judging tissue hardness by palpation.

Funding

This work was supported by JSPS KAKENHI Grant Numbers 24500520, 17K01536.

Conflicts of interest

The authors have no conflicts of interest to declare regarding this study.

REFERENCES

1) Vernon H, Gitelman R: Pressure algometry and tissue compliance measures in the treatment of chronic headache by spinal manipulation: a single case/single treatment report. J Can Chiropr Assoc, 1990, 34: 141–144.
2) Horikawa M, Ebihara S, Sakai F, et al.: Non-invasive measurement method for hardness in muscular tissues. Med Biol Eng Comput, 1993, 31: 623–627. [Medline] [CrossRef]
3) Komiya H, Maeda J, Takemiya T: A new functional measurement of muscle stiffness in humans. Adv Exerc Sports Physiol, 1996, 2: 31–38.
4) Vannah WM, Childress DS: Indentor tests and finite element modeling of bulk muscular tissue in vivo. J Rehabil Res Dev, 1996, 33: 239–252. [Medline]
5) Pathak AP, Silver-Thorn MB, Thierfelder CA, et al.: A rate-controlled indentor for in vivo analysis of residual limb tissues. IEEE Trans Rehabil Eng, 1998, 6: 12–20. [Medline] [CrossRef]
6) Leonard CT, Deshner WP, Romo JW, et al.: Myotonometer intra- and interrater reliabilities. Arch Phys Med Rehabil, 2003, 84: 928–932. [Medline] [CrossRef]
7) Kato G, Andrew PD, Sato H: Reliability and validity of a device to measure muscle hardness. J Mech Med Biol, 2004, 4: 213–225. [CrossRef]
8) Rydahl SJ, Brouwer BJ: Ankle stiffness and tissue compliance in stroke survivors: a validation of myotonometer measurements. Arch Phys Med Rehabil, 2004, 85: 1631–1637. [Medline] [CrossRef]
9) Arokoski JP, Surakka J, Ojala T, et al.: Feasibility of the use of a novel soft tissue stiffness meter. Physiol Meas, 2005, 26: 215–228. [Medline] [CrossRef]
10) Ylinen J, Teittinen I, Kainulainen V, et al.: Repeatability of a computerized muscle tonometer and the effect of tissue thickness on the estimation of muscle tone. Physiol Meas, 2006, 27: 787–796. [Medline] [CrossRef]
11) Kinoshita H, Miyakawa S, Mukai N, et al.: Measurement of tissue hardness for evaluating flexibility of the knee extensor mechanism. Footb Sci, 2006, 3: 15–20.
12) Moromugi S, Kumano S, Ueda M, et al.: A sensor to measure hardness of human tissue. 5th IEEE Conference on Sensors, 2006, 388–391.
13) Gubler-Hanna C, Laskin J, Marx BJ, et al.: Construct validity of myotonometric measurements of muscle compliance as a measure of strength. Physiol Meas, 2007, 28: 913–924. [Medline] [CrossRef]
14) Lidström A, Ahlsten G, Hirchfeld H, et al.: Intrarater and interrater reliability of myotonometer measurements of muscle tone in children. J Child Neurol, 2009, 24: 267–274. [Medline] [CrossRef]
15) Morozumi K, Fujiwara T, Karasuno H, et al.: A new tissue hardness meter and algometer; a new meter incorporating the functions of a tissue hardness meter and an algometer. J Phys Ther Sci, 2010, 22: 239–245. [CrossRef]
16) Morozumi K, Morishita K, Aoki M, et al.: Investigation of absolute intra-rater and inter-rater reliabilities during the muscle hardness estimation. J Phys Ther Sci, 2022, 34: 122–130. [Medline] [CrossRef]
17) Gefen A, Megido-Ravid M, Azariah M, et al.: Integration of plantar soft tissue stiffness measurements in routine MRI of the diabetic foot. Clin Biomech (Bristol, Avon), 2001, 16: 921–925. [Medline] [CrossRef]
18) Suga M, Matsuda T, Minato K, et al.: Measurement of in-vivo local shear modulus by combining multiple phase offsets mr elastography. Stud Health Technol Inform, 2001, 84: 933–937. [Medline]
19) Dresner MA, Rose GH, Rossman PJ, et al.: Magnetic resonance elastography of skeletal muscle. J Magn Reson Imaging, 2001, 13: 269–276. [Medline] [CrossRef]
20) Basford JR, Jenkyn TR, An KN, et al.: Evaluation of healthy and diseased muscle with magnetic resonance elastography. Arch Phys Med Rehabil, 2002, 83: 1530–1536. [Medline] [CrossRef]
21) Uffmann K, Maderwald S, Ajaj W, et al.: In vivo elasticity measurements of extremity skeletal muscle with MR elastography. NMR Biomed, 2004, 17: 181–190. [Medline] [CrossRef]
22) Nordez A, Hug F: Muscle shear elastic modulus measured using supersonic shear imaging is highly related to muscle activity level. J Appl Physiol, 2010, 108:

1389–1394. [Medline] [CrossRef]
23) Lacourpaille L, Hug F, Bouillard K, et al.: Supersonic shear imaging provides a reliable measurement of resting muscle shear elastic modulus. Physiol Meas, 2012, 33: N19–N28. [Medline] [CrossRef]
24) Chino K, Akagi R, Dohi M, et al.: Reliability and validity of quantifying absolute muscle hardness using ultrasound elastography. PLoS One, 2012, 7: e45764. [Medline] [CrossRef]
25) Yavuz A, Bora A, Bulut MD, et al.: Acoustic Radiation Force Impulse (ARFI) elastography quantification of muscle stiffness over a course of gradual isometric contractions: a preliminary study. Med Ultrason, 2015, 17: 49–57. [Medline] [CrossRef]
26) Nakayama M, Ariji Y, Nishiyama W, et al.: Evaluation of the masseter muscle elasticity with the use of acoustic coupling agents as references in strain sonoelastography. Dentomaxillofac Radiol, 2015, 44: 20140258. [Medline] [CrossRef]
27) Hai P, Zhou Y, Gong L, et al.: Quantitative photoacoustic elastography in humans. J Biomed Opt, 2016, 21: 66011. [Medline] [CrossRef]
28) Hai P, Zhou Y, Gong L, et al.: Quantitative photoacoustic elastography of Young's modulus in humans. SPIE BiOS, 2017, 10064: 100640B.
29) Karayol KC, Karayol SS: A comparison of visual analog scale and shear-wave ultrasound elastography data in fibromyalgia patients and the normal population. J Phys Ther Sci, 2021, 33: 40–44. [Medline] [CrossRef]
30) Feng YN, Li YP, Liu CL, et al.: Assessing the elastic properties of skeletal muscle and tendon using shearwave ultrasound elastography and MyotonPRO. Sci Rep, 2018, 8: 17064. [Medline] [CrossRef]
31) Zheng Y, Mak AF: Effective elastic properties for lower limb soft tissues from manual indentation experiment. IEEE Trans Rehabil Eng, 1999, 7: 257–267. [Medline] [CrossRef]
32) Then C, Menger J, Benderoth G, et al.: A method for a mechanical characterisation of human gluteal tissue. Technol Health Care, 2007, 15: 385–398. [Medline] [CrossRef]
33) Isogai K, Okamoto S, Yamada Y, et al.: Skin-fat-muscle urethane model for palpation for muscle disorders. IEEE/SICE International Symposium on System Integration, 2015, 960–964.
34) Akoglu H: User's guide to correlation coefficients. Turk J Emerg Med, 2018, 18: 91–93. [Medline] [CrossRef]